University of Texas at El Paso

ScholarWorks@UTEP

2023-08-01

Performance Evaluation Of A Coupled Photovoltaic-Thermal Solar Powered Desalination Pilot System

Martin Chavarin
University of Texas at El Paso

PERFORMANCE EVALUATION OF A COUPLED PHOTOVOLTAIC-THERMAL SOLAR

POWERED DESALINATION PILOT SYSTEM

MARTIN CHAVARIN

Master's Program in Environmental Engineering

APPROVED:

W. Shane Walker, Ph.D., Chair

Ivonne Santiago, Ph.D.

Malynda Capelle, Ph.D.

Stephen L. Crites, Jr., Ph.D.
Dean of the Graduate School

DEDICATION

This thesis is dedicated to Socorro Mendez, my mother.

PERFORMANCE EVALUATION OF A COUPLED PHOTOVOLTAIC-THERMAL SOLAR

POWERED DESALINATION PILOT SYSTEM

by

MARTIN CHAVARIN, B.S.

THESIS

Presented to the Faculty of the Graduate School of

The University of Texas at El Paso

in Partial Fulfillment

of the Requirements

for the Degree of

MASTER OF SCIENCE

Department of Civil Engineering

THE UNIVERSITY OF TEXAS AT EL PASO

August 2023

ACKNOWLEDGEMENTS

ABSTRACT

A pilot scale coupled photovoltaic-thermal solar powered desalination system was evaluated at the Brackish Groundwater National Desalination Research Facility (BGNDRF). The pilot system consisted of a 3-kW photovoltaic-thermal (PVT) solar panel array and a 2.3 kW photovoltaic (PV) array coupled with a 4 gal/min single-stage 4 membrane reverse osmosis (RO) desalination system. A heat exchange system was in place to provide simultaneous cooling for the PVT system and heating to the RO system feed water.

This system was evaluated with three objectives in mind. The first objective was to identify whether cooling of the PVT panels resulted in a significant increase in energy production. Increased operating temperatures in PV panels result in decreased electrical conversion efficiencies. The second objective was to evaluate an increase in total daily permeate production when the heat exchange system was in operation and the feed water tank was heated. Higher feed water temperatures result in lower viscosity in the feed water allowing for increased water production. The third objective was to evaluate the impact of greater feed water temperature on permeate water quality. Higher feed water temperatures result in an increase in salt passage.

The heat exchange system did result in lower operating temperatures in the PVT system, a significant increase in energy production was not immediately apparent, but rather a decrease in energy production was noticed. With the heat exchange on, a mean RO feed water temperature increase of 3.8°F during daylight hours (7 AM to 7 PM) was associated with a 0.8% increase in total daily permeate production. Permeate water conductivity was analyzed to evaluate the change in permeate water quality when the heat exchange system was on. Although an increase in conductivity was identified, it was not substantial enough to conclude that heating of the feed water to the system resulted in a significant increase in salt passage.

TABLE OF CONTENTS

LIST OF FIGURES

INTRODUCTION

Background

The water crisis facing the world in the 21st century is being driven by factors including urbanization, climate change, and pollution. Water scarcity affecting global urban populations is projected to increase by 122% from 2016 to 2050, up to an estimated 2.1 billion people globally (He et al., 2021). Other models have projected that up to 4.3 billion people currently experience moderate to severe water scarcity for at least one month of the year (Mekonnen & Hoekstra, 2016). As water scarcity is exacerbated due to water quality and water quantity issues, it is imperative to study and evaluate technologies which improve access to clean and safe drinking water around the world.

Desalination has been identified as a potential solution to water scarcity, among other methods such as groundwater exploitation, reservoir construction, and inter-basin water transfer (He et al., 2021). Groundwater exploitation is unsustainable, reservoirs increase water loss due to evaporation, and inter-basin water transfers may be prohibitively costly. While desalination opens up new water sources, desalination lies at the center of the water-energy nexus, with energy contributing to 35-50% of the operational costs of desalination plants. High energy costs have kept desalination out of reach for communities globally, especially for developing and underdeveloped countries (Goh et al., 2017). Reverse osmosis (RO) is one of the most energy-efficient desalination processes for brackish water, and it uses mechanical pressure (exceeding the osmotic pressure) to force water through the RO membrane, which rejects most of the dissolved salts.

Renewable energy sources such as photovoltaic (PV) have recently become cost-competitive with conventional power and now may be a viable option to power desalination

systems. Solar energy has an enormous potential for power generation: the earth receives close to four million exajoules of energy from the sun, of which five thousand are easily harvestable(Kabir et al., 2018). In terms of averaging the solar irradiance of 1361 W/m^2 over the surface of the globe, annually, close to 342 W/m^2 is received, of which 70% is available for harvesting (Kabir et al., 2018). A correlation can be made between regions facing severe water scarcity and regions with higher levels of photovoltaic power potential, such as the southwest region of the United States. The average daily solar irradiance in the southwestern United States ranges between 5.5 to greater than 7.5 kWh/m^2 (Sengupta et al., 2018).

Solar energy collection systems can be divided into two categories, passive solar technologies, and active solar technologies. Passive solar technologies involve the collection of solar energy without transforming it into other forms of energy and include direct, indirect, and isolated solar gain. Active solar technologies collect solar radiation and convert it to heat and electrical power with the help of mechanical and electrical equipment (Kabir et al., 2018). Active solar technologies can be grouped into two categories, photovoltaic and solar thermal technologies (Kabir et al., 2018). PV has become a predominant technology for renewable energy in the recent past and has shown exponential growth in both development and market share (Tiwari et al., 2011). PV cells allow for the conversion of solar energy into electricity using semiconductor materials using the photovoltaic effect. Several methods and materials are currently available to produce PV cells, however the PV market is currently dominated by crystalline silicon. Emerging technologies such as thin film silicon and organic solar cells have produced promising results in performance and cost (Tiwari et al., 2011).

One of the major drawbacks of PV technologies is underperformance when it comes to performance and reliability. A study performed by the National Renewable Energy Lab (NREL)

in 2015 evaluated 20 commercially available PV modules for performance and efficiency. The highest efficiency obtained from the study was 19.3% from a Sunpower 315 module using monocrystalline silicon PV cells. PV systems' reliability and durability have also fallen short due to exposure to varying environmental conditions during their lifetime(Waqar Akram et al., 2022).

Dr. Malynda Cappelle and the late Dr. Tom Davis patented the synergistic combination of photovoltaic thermal (PVT) with desalination (Figure 1). PVT panels produce electricity and recover heat from the solar irradiance, and when a heat exchanger is used to transfer the heat from the panels to the desalination feedwater, two benefits occur: the panels are cooler, which increases their energy efficiency, and the feedwater is warmer, which decreases the energy required for desalination, either by RO or electrodialysis (ED).
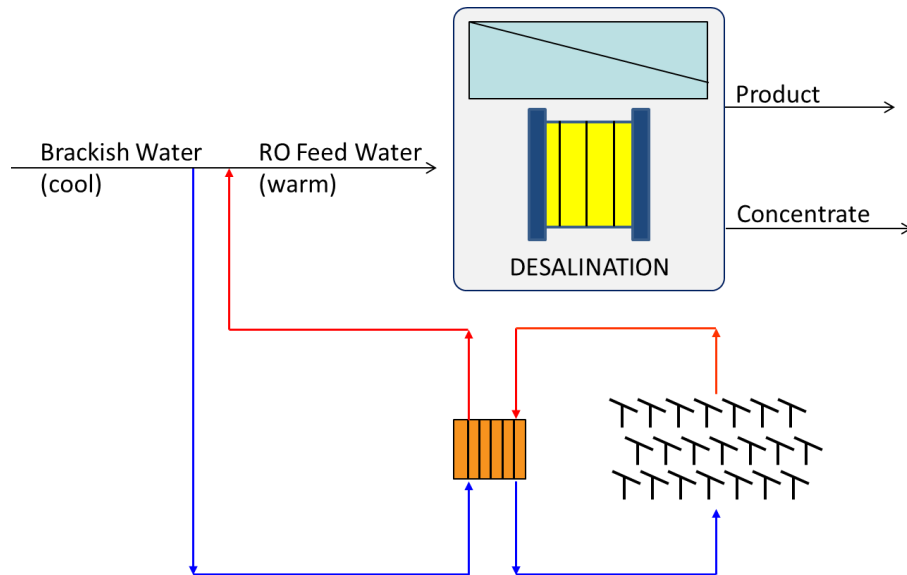
Figure credit: Dr. Malynda Cappelle

Figure 1. Conceptual diagram of coupled PVT-RO system

Objectives

The goal of this study was to evaluate the performance of a pilot scale PVT RO brackish groundwater desalination system. The three main research questions were:

1. To what extent does the cooling of the PVT panels in combination with the desalination system increase their energy production?

2. To what extent does the corresponding increase in the feed water temperature in a RO desalination increase total water production at a constant feed pump setpoint?

3. To what extent does the product water salinity increase when implementing a heat exchange system to increase RO feed water temperature?

METHODOLOGY

The UTEP pilot system shown in Figure 2 is located at the Brackish Groundwater National Desalination Research Facility (BGNDRF). BGNDRF is a facility in Alamogordo, New Mexico, managed by the U.S. Department of Interior's Bureau of Reclamation, and it provides brackish groundwater from four different wells in the northern section of the Hueco-Mesilla Bolson, also known as the Tularosa Basin. BGNDRF hosts entities looking to pursue research in desalination, including concentrate management solutions, hybrid renewable energy desalination systems, and small-scale desalination systems, among other desalination-related research topics. Water from Well 1 is directed to this pilot trailer which is powered by two solar panel arrays, a photovoltaic-thermal array, and a conventional photovoltaic array, and consists of a single-pass, single-stage, 4-element membrane desalination system that includes antiscalant dosing and incorporates a heat exchange system at the feed tank.

Figure 2. PVT Pilot at BGNDRF

Evaluation on the PVT-RO system began in January 2021 with the review of historical data as well as planning for a restart of the system. In July of 2021, the battery system was upgraded from saltwater batteries to a lithium iron phosphate battery. The RO membranes were replaced in August of 2021, and the system was restarted in August 2021. In February of 2022, a

leak in the glycol system was identified and repaired. Troubleshooting to replace the empty glycol loop took place in June of 2022. In August 2022, flow meters for the feed permeate, and concentrate streams were installed to replace the system totalizers which were notorious for sporadic data reporting. New NF270 membranes were installed in August of 2022, and the system was restarted (again). The evaluation period for this study was from August 18 to October27. 2022, after which the pilot began receiving a mixture of water from Well 1 and Well 3.

PV and PVT

Power to the system was entirely provided by renewable solar energy using a combination of PVT and PV panel arrays. The PVT panel array consisted of 16 WIOSUN 180W PV-Therm Modules from Solar Zentrum with a gross area of 224 ft² (20.8 m²). The modules provided a total peak power output of 2.88 kW. The panels were mounted on an OSPREY Solar Air Ground Mount Power Platform System from Nuance Energy with Earth Anchor, and they were set to a collector tilt angle of 30 degrees and with an azimuth at 180 degrees, or "true south." The supplemental PV portion of the power system consisted of nine CanadianSolar CS6P-255P panel array with a gross area of 104 ft² (9.7 m²), each with a nominal peak power output of 255 W for up to 2.3 kW of additional electrical power to the desalination system. The total combined rated electrical power from the PVT and PV arrays is 4.41 kW.

Figure 3 below shows the total daily electrical energy production of the PV and PVT systems during the evaluation period between 8/18/22 to 10/27/22. ON and OFF operations of the heat exchanger are labeled in Figure 3.
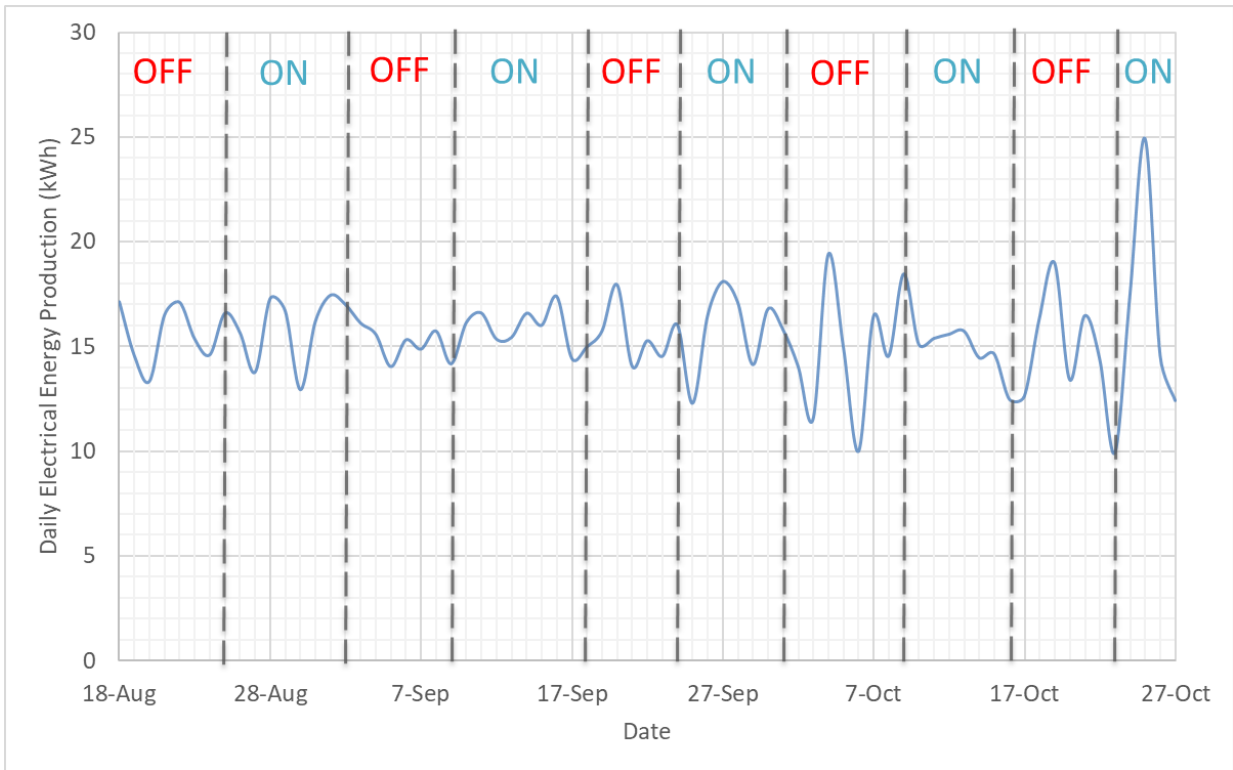
Figure 3. Combined PV and PVT Daily Electrical Energy Production During ON/OFF Heat Exchange Operation

Electrical Power Management

A Schneider Electric 865-4048 Context SW split phase 120/240 inverter/charger managed electrical power. The Context SW had an inverter output power of 3400 W and a peak current of 41 A, with optimal efficiency of 92%. It had a charging output current of 90 A and a nominal output voltage of 48VDC, with an optimal efficiency of 90%. The system also included four Schneider Electric Context MPPT 60 PV solar charge controllers with a maximum power output of 3500 W and a maximum power conversion efficiency of 98% at 48V. Electrical power storage was provided by a Fortress Power eVault 1.5 Lithium Iron Phosphate battery with a nominal voltage of 51.2 V and a nominal charge capacity and energy storage of 360 Ah and 18.5 kWh, respectively. Battery and solar performance were monitored using the accompanying Schneider Electric monitoring software Insight Cloud. Insight Cloud provided live updates for

7

the system power flow, solar production, energy consumption, load, and battery charging and discharging values.

Nanofiltration System

The desalination system evaluated in this pilot used brackish groundwater from Well 1 of the BGNDRF as its feed water source. Well one was used due to the lower salinity (e.g., approximately 1 g/L total dissolved solids) compared to other BGNDRF wells, and the lack of contamination by per- and poly-fluoroalkyl substances (PFAS).

The feed water to the system was controlled by a float-controlled solenoid valve; the system used a 140-gallon feed tank, and the raw feed valve was opened when the level reached 120 gallons. Simultaneously, the antiscalant dosing pump would turn on and feed the antiscalant to the feed tank while refilling to a water level of 140 gallons. The antiscalant used in this study was Avista Vitec 7000, diluted to a stock solution of 10% of the original concentration. The dosing rate of the pump is set such that the final feed water antiscalant concentration will be approximately four parts per million by volume.

The membrane desalination system incorporated four Dupont Filmtec NF270-4040 membranes configured as a single-pass, single-stage, four-element system. The pump used to power the system was a WEBTROL G5B10S16T EZ Series 0.5 HP single-phase booster pump with a variable frequency drive (VFD) with a maximum frequency of 60 Hz. The VFD was set at a constant value of 45Hz to provide approximately 50% system recovery with a feed flow rate of 4-4.5 GPM. The system permeate was directed to an overflow tank with a capacity of 50 gallons, then directed into the municipal drainage. Concentrate from the desalination system was also directed into municipal drainage.

Heat Exchange System

The heat exchange system was powered by a PAW pump station which included a 2-gallon AMTROL Solar Extrol expansion tank. Dynalene Solar Glycol XT was used as the heat transfer fluid in the heat exchange system. It is a sustainable and bio-based heat transfer fluid. It provides an operating temperature range of -17°F to 350°F, which was more than sufficient for the expected operating conditions of the pilot system. The flow rate of the heat transfer fluid was set at 2 gal/min. Supply and return piping of the heat exchange system consisted of blue(supply) and red(return) Sharkbite PEX pipe, which was flexible and freeze resistant. The supply line carried the cooled glycol liquid to the PVT panel arrays, exiting into the return line that fed into the heat exchange coils in the feed tank. The heat exchange coils were made of approximately 10 ft (3 m) of 1-inch diameter ribbed stainless steel flexible tubing for a total external heat transfer surface area of 2.6 ft² (.25 Q m²).

The accompanying thermal-grid software provided control and site monitoring of the heat exchange system. One thermal grid DL2 was used to send data to the servers, and one RESOL Deltasol BS Plus controller worked in conjunction with a RESOL WMZ-Full Kit system to provide operating controls to the system. The thermal grid software allowed adjustment of pump operation and speed settings, and temperature setpoints when the system was in the automatic setting. The temperature settings are the temperature differentials between the feed and array tank temperatures. These differentials were used to control when the heat exchange pump turned on and off. The heat exchange system turned on at a temperature differential of 5.4°F and turned off at a temperature differential of 1.8°F. It also allowed us to control the maximum storage tank temperature, set approximately 110°F, to abide by the maximum operating temperatures of the NF270 membranes.

Figure 4 below shows the daily average ambient temperatures at the pilot location during the evaluation. Figure 4. is labeled to show when the heat exchange system was turned on. Figure 4 shows the statistical distribution of the temperatures between ON and OFF periods.
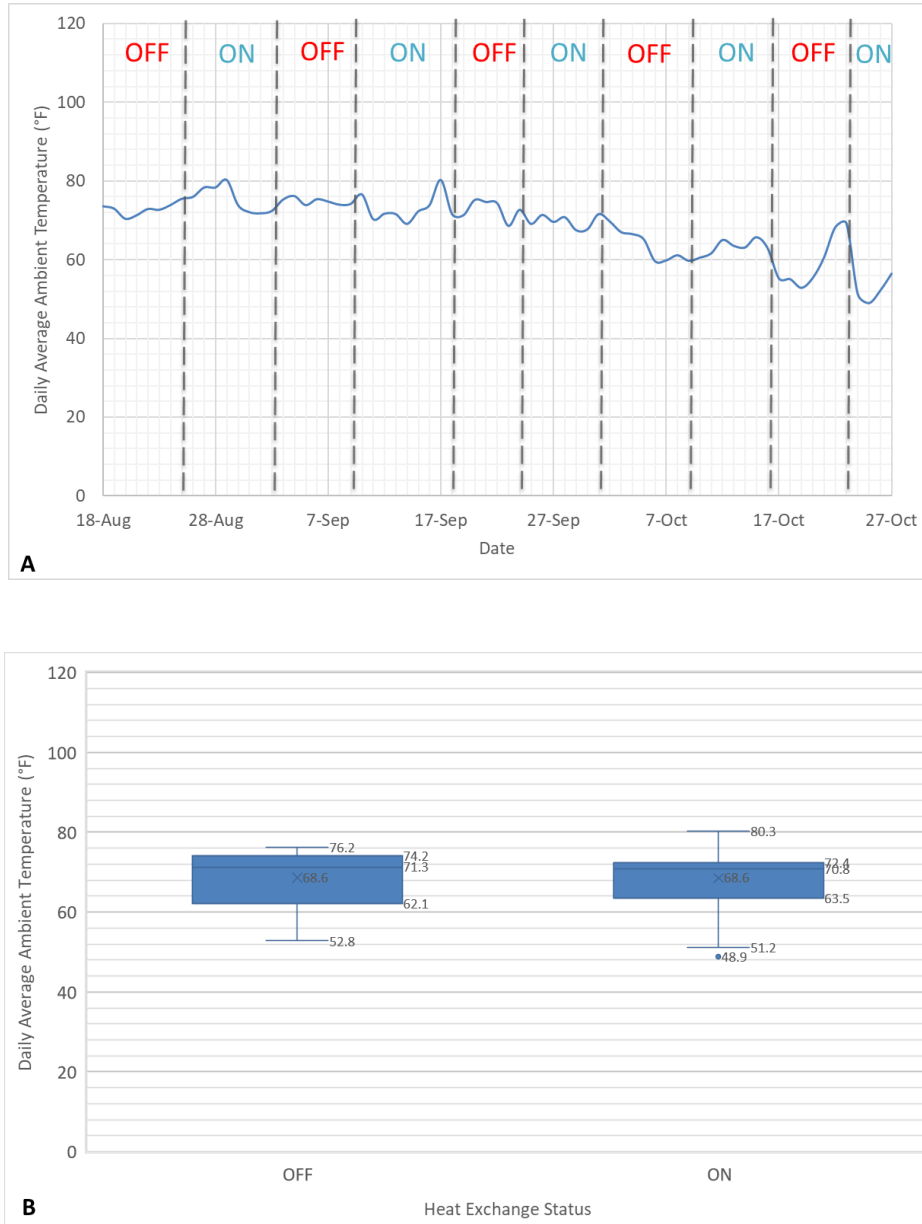

Figure 4. A) Daily average ambient temperature with ON/OFF heat exchange periods labeled B) Daily average ambient temperature distributions during ON/OFF heat exchange periods.

10

Data Collection

Data were collected from several sources, depending on which data type was to be collected. NF/RO operations data were gathered from the programmable logic controller (PLC) and human machine interface (HMI) system setup by Industrial Water Services (IWS) of El Paso (desalination equipment manufacturer) and included operating pressures, temperatures, flow rates, conductivities, and temperatures. Solar and thermal power data were collected using the Thermal Grid software and included system temperatures, flow rates, thermal and electrical production, ambient temperatures, and system activity status. Electrical and battery data were collected using the Insight Cloud software and included system solar production, energy consumption, load, and battery charging and discharging values.

Water Quality Analysis

Water samples were collected and analyzed for the system feed tank, system permeate, and system concentrate. On-site water quality analyses included pH and conductivity measurements. Measurements for the pH and conductivity were performed using a ThermoScientific ORION Star A323 meter which was calibrated for both pH and conductivity. The system's HMI interface also supplied live readings of the raw, tank, permeate, and concentrate stream conductivities, as well as their respective flow rates and pressures. Further water quality analyses were performed at the UTEP CIDS water quality analysis lab and included measurements for alkalinity, total dissolved solids, and silica concentrations.

Alkalinity was measured with a Microlab FS-522 using a titration method that dosed 0.02 N sulfuric acid to the sample. The experiment measured pH using the same probe used for on-site pH analysis. The dosing of acid ended when the sample had a measured pH value of 3.5. The intersection value between the measured and theoretical pH was used as the final alkalinity

measurement of the sample. This method included a standard check of 100 mg/L alkalinity as $CaCO_3$ using 168 mg/L of $NaHCO_3$.

Total dissolved solids (TDS) were measured using the standard TDS gravimetric method for water quality analysis. The sample is first filtered through a 0.45-micron filter, then placed in an aluminum weighing dish and set to bake at 180°C. The dish's initial dry weight and the dish's dry weight with the dried sample were measured and used to calculate the final TDS concentration.

Silica analysis was performed using the HACH DR 5000 Spectrophotometer and HACH Method 8185. This method uses molybdate, acid, and citric acid reagents to measure silica concentration. A blank of the sample is first measured to attain a zero value, and then the sample with the reagents added is measured to obtain the final silica concentration of the sample.

Ion chromatography analysis was also performed for the samples. Ion chromatography analyzed both anion and cation concentrations in the samples. A Dionex Integrion and Dionex Acquion were used for anion and cation chromatography analysis, respectively. The anion analysis method used the Dionex Integrion with a 4mm IonPac AS18 analytical column and 30 mM potassium hydroxide eluent to analyze chloride, fluoride, nitrate, nitrite, and sulfate ion concentrations. The cation analysis method used the Dionex Acquion with a 5mm IonPac CS16 analytical column and 47 mM methanesulfonic acid to analyze calcium, potassium, magnesium, sodium, lithium, and ammonium ion concentrations. The results were processed and analyzed using the accompanying Chromeleon Chromatography Data System Software, and final ion concentrations were reported in mg/L.

Data Management and Analysis

The RO system records minute-by-minute conductivity measurements and flow rates in individual *txt* files, saved and updated as individual daily files. These files were appended into a single file of desalination data in Python, where calculated variables were also added to the data set, such as standard and specific flux. Osmotic pressure for the RO system was calculated with an assumed phi value of 0.97. Using that osmotic pressure calculation, specific flux was calculated for each minute.

The solar system records Total Energy Produced per hour, recording data at the top of every hour. Therefore, the desalination data was aggregated to hourly median values for all reported and calculated variables. The solar data was then merged onto the desalination data set using both systems' date and time stamps as a key.

PV and PVT Energy Production

One the benefits of having a supplementary traditional PV system is that it allows us to monitor and obtain baseline PV performance values. Since the traditional PV system performance is not dependent on the heat exchange system, the production values can be used to monitor variability between OFF and ON periods of the heat exchanger. It was expected that PV energy production values would show little to no variability between OFF and ON periods. The statistical distributions of daily PV production values are summarized in box and whisker plots[1] in Figure 5. The mean daily PV production values when the heat exchange was OFF vs ON were 5.93 and 5.74 kWh/day, with median values at 5.72 and 5.77 kWh/day, respectively. Analysis of the PV energy production values shows a 3.3% difference in mean values and 0.8% difference in median values between OFF and ON periods. So, there is a negligible difference in PV energy production when comparing median values.

---

[1] The whiskers show the maximum (100th percentile) and minimum (0th percentile), the box shows the 75th percentile and 25th percentile, and the horizontal line and "x" represent the median (50th percentile) and arithmetic mean ("average"), respectively. Statistical outliers are shown as individual points outside of the range of the whiskers.
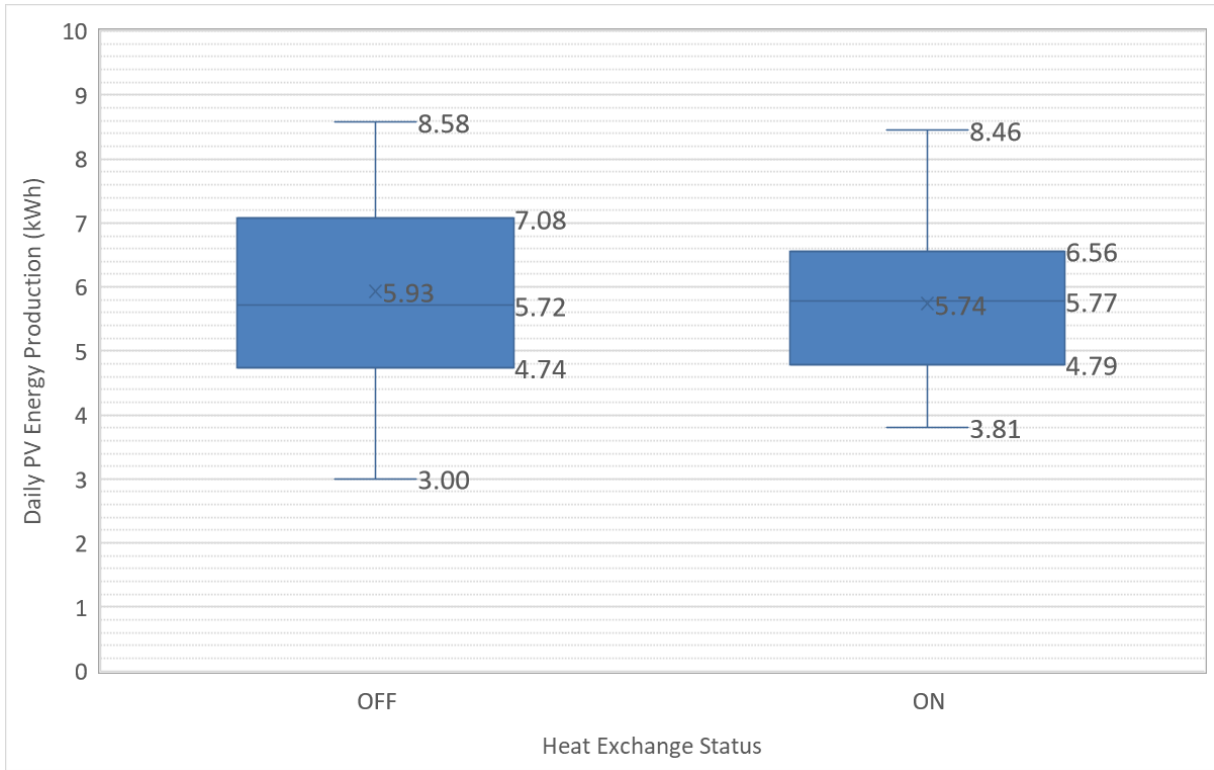
Figure 5. Daily PV energy production, without and with PVT heat exchange

The statistical distributions of daily PVT energy production for OFF and ON periods of the heat exchanger are summarized in Figure 6. Expected results for the PVT system were for energy production to increase when the heat exchange system was on because lower operating temperatures of the PVT modules should increase the energy production efficiency. The mean PVT energy production when the system was OFF and ON was 9.14 and 9.90 kWh/day, and median values were 9.70 and 10.47 kWh/day, respectively. When comparing the mean and median values, the daily PVT energy increased. Median PVT energy production was 7.9% greater during the ON periods vs OFF periods.
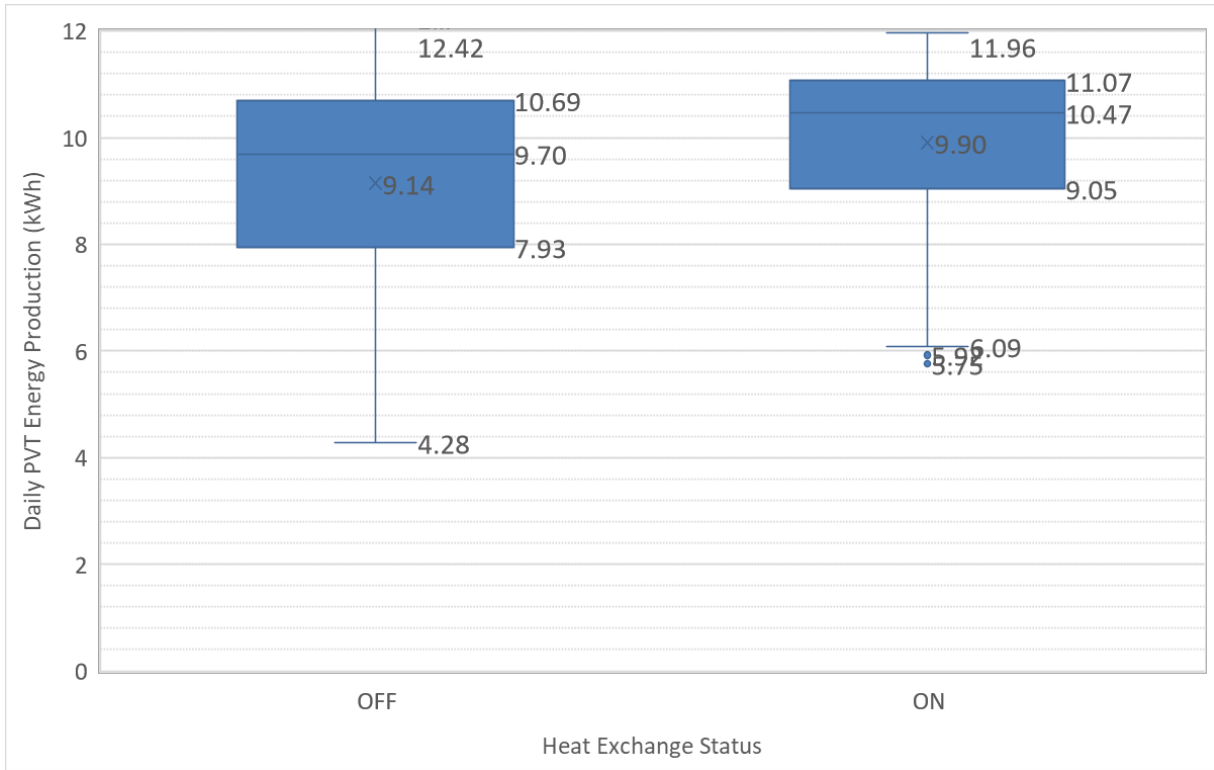
Figure 6. Daily PVT Energy Production, without and with PVT heat exchange

PVT Operating Temperature

The statistical distribution of the hourly average operating temperatures of the PVT panels during OFF and ON periods of the heat exchanger are summarized in Figure 7. The heat exchange system works by directing cooled glycol liquid to the PVT panels, which effectively lowers the operating temperature of the PVT panels by exchanging the heat from the panels to the glycol liquid. The operating temperature when the heat exchange system was in operation was lower, with mean operating temperatures at 103.0 °F with the heat exchange system off and 90.7 °F with the heat exchange system on, and median temperatures at 100.2 °F and 92.6 °F, respectively. Thus, the heat exchange system appeared to be cooling the panels to reduce the average daily temperature by 12.3 °F and the median daily temperature by 7.6 °F compared to when the heat exchange system was off. Accounting for the PV baseline difference of 0.8%, the

PVT energy production increase of 7.1% due to operation of the heat exchange corresponds to nearly 1% increase in energy production observed per °F cooled.
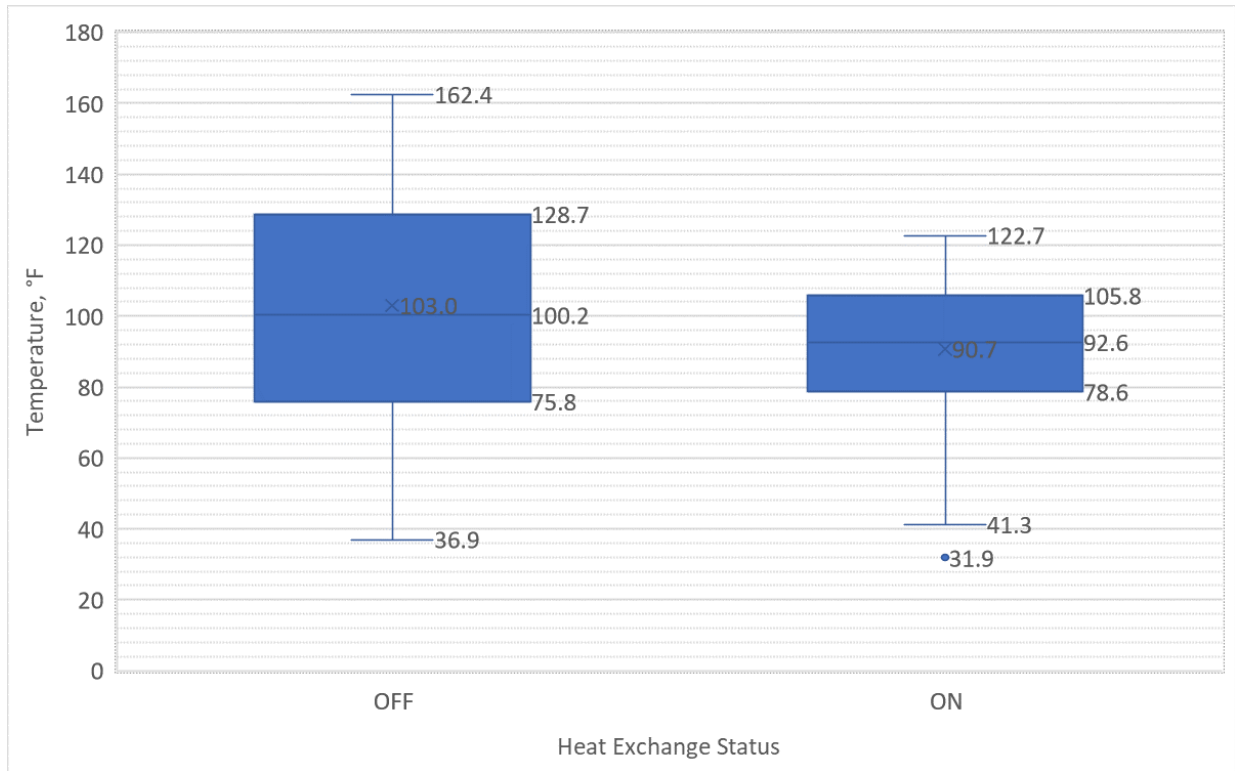

Figure 7. Operating PVT Panel Temperature

RO Feed Operating Temperature

As the glycol loop runs through the PVT panels, it is heated and redirected to the RO system feed tank where the heat exchange coil is located. As the heated glycol liquid circulates through the RO system feed tank, the temperature of the water is expected to increase. The am to 7 pm, statistical distributions of average hourly temperatures during daylight hours between of the RO system feed tank during the testing period are summarized in Figure 8. The average hourly feedwater temperature was higher when the heat exchange system was in operation. Mean values for OFF and ON periods were 81.3 °F and 77.6 °F, and median values were 78.7 °F and

17

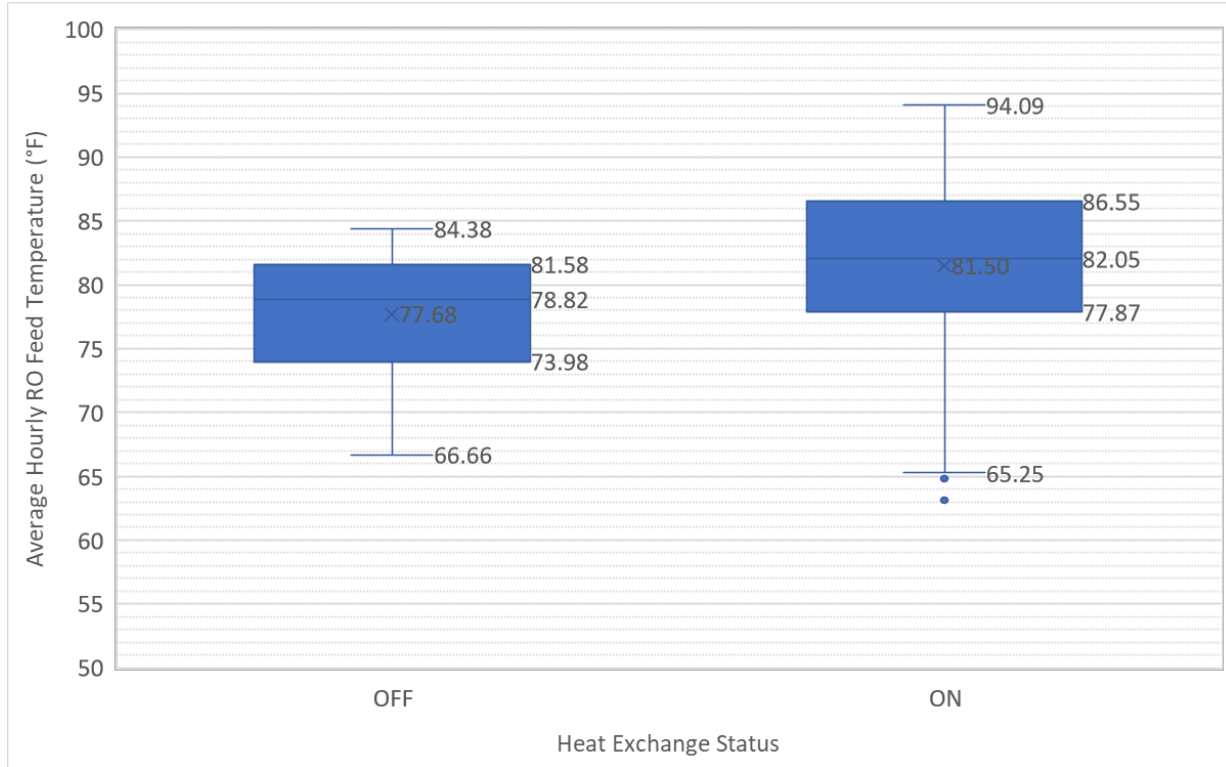81.6 °F, respectively. Median feed temperature was 3.2 °F higher during ON periods.

Figure 8. Average Hourly RO Feedwater Temperature

Water Production

Statistical distributions of daily RO permeate water production are shown in Figure 9. Permeate production was greater when the heat exchange system was ON, with mean daily production of 3169 gallons and median daily production of 3193 gallons with the heat exchange system OFF and 3197 and 3206 gallons, respectively, with the heat exchange system ON. Thus, the RO system produced approximately 0.8% or 0.4% more permeated with the heat exchange system when comparing the mean and median values, respectively.
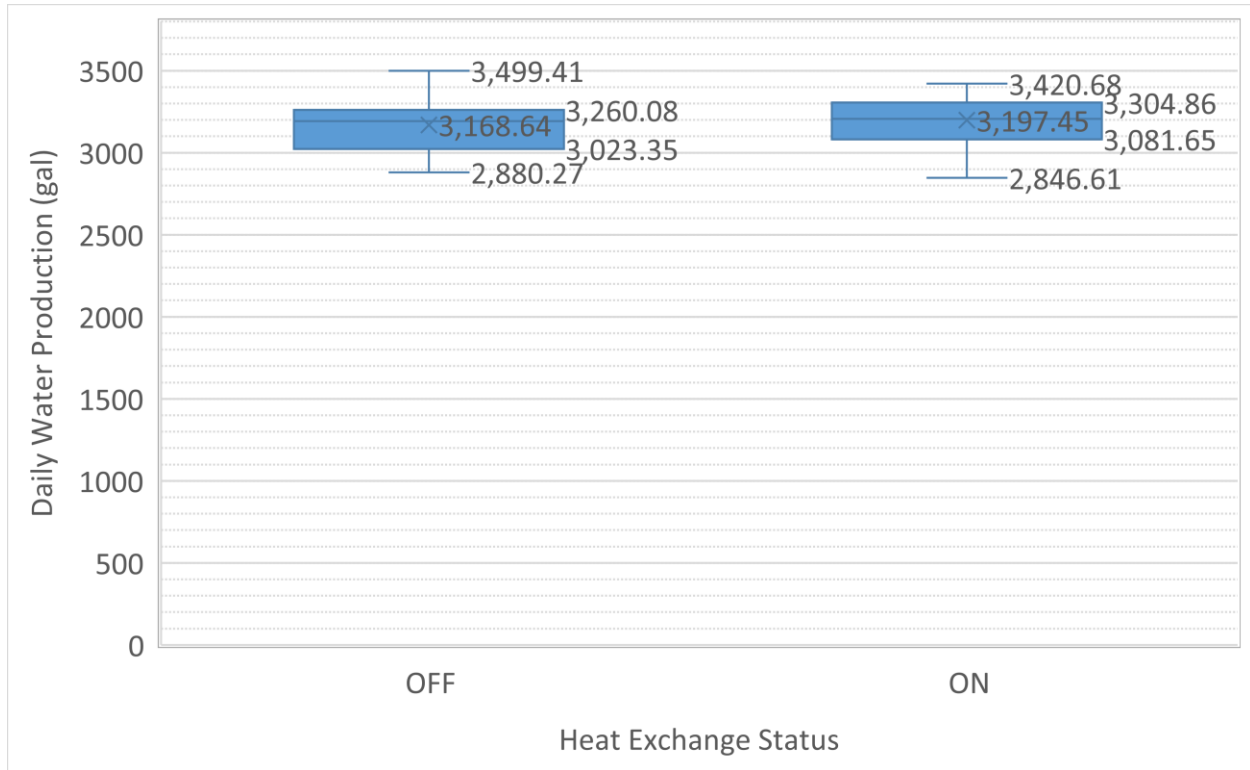
18

Figure 9. Daily System Water Production

Conductivity

Statistical distributions of conductivity values for the feed, permeate, and concentrate streams of the RO system are summarized in Figure 10. It is expected that when the feedwater temperature is warmer, the RO membrane will exhibit greater salt passage, so the permeate conductivity would be higher when the heat exchange is on. The mean feed conductivity values were 1672 µS/cm when the heat exchange was off and 1670 µS/cm with the heat exchange on, with median values of 1678 and 1675 µS/cm, respectively. Thus, the system feed water quality remained very consistent throughout the testing period when the system was on as well as off. By analyzing the permeate conductivity variability, we can also see how the increase in feed water temperature affected permeate water quality. The maximum and 75th percentile values of the permeate conductivity when the heat exchange is on are 1.0% and 0.2% greater, respectively,

19

than when the system is off. However, mean, and median values decrease when the heat exchange is on, but those values were impacted by night-time ambient temperatures when the heat exchange loop would not be operating.
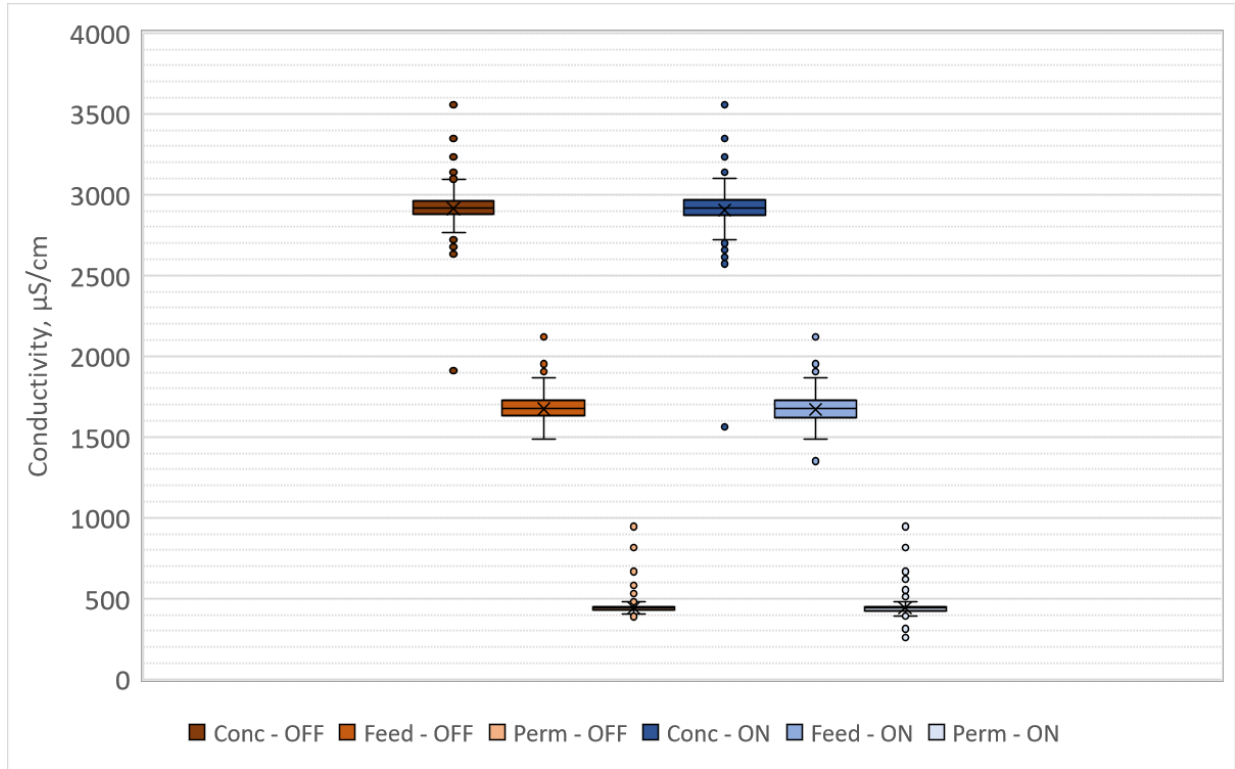

Figure 10. System Conductivity for Feed, Permeate, and Concentrate Streams

Samples were collected and prepared for ion chromatography analysis from the feed, permeate, and concentrate streams. Figure 11 shows the statistical distribution of sodium, calcium, and magnesium cations, as well as chloride, sulfate, and alkalinity for anions. Ion chromatography results show a similar pattern between concentration distributions for OFF and ON periods compared to conductivity. Calcium, magnesium, and sulfate were rejected well by the NF270 membranes, with sulfate having the highest rejection. Mean sodium distribution shows approximately 70% removal when heat exchange system is ON, and 71% removal when heat exchange is off. No substantial differences in ion rejection were observed due to the temperature difference between heat exchange conditions.
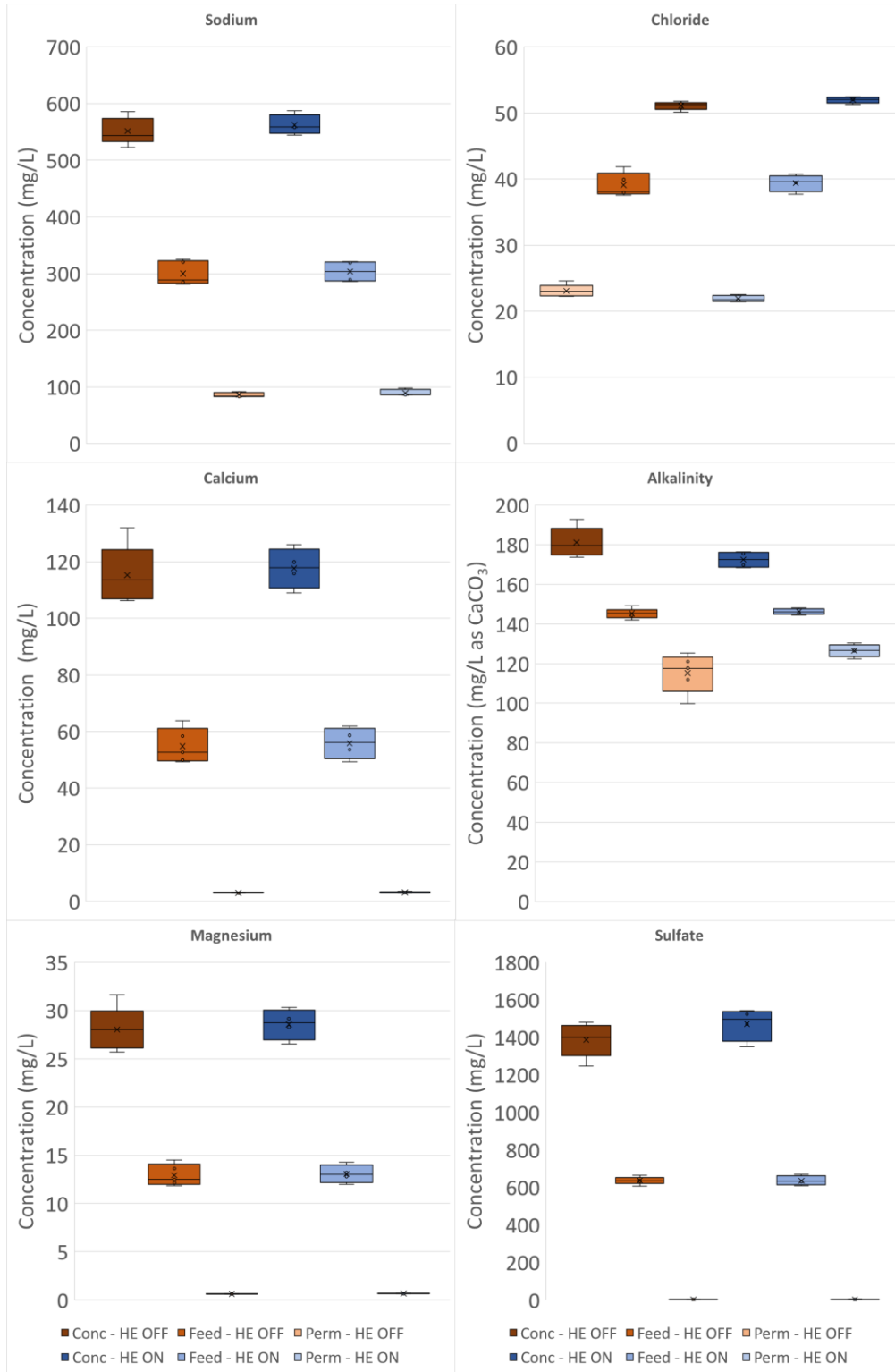
20

Figure 11. Concentrations of ionic constituents in concentrate, feed, and permeate, during OFF an ON heat exchange periods.

CONCLUSION

A coupled PVT-RO pilot desalination system was successfully evaluated over an 8-week period at the BGNDRF. Approximately 4 gal/min of BGNDRF Well 1 was provided as feed water for a single-stage RO desalination system operating at approximately 50% recovery. The system was powered by a 3 kW PVT solar panel array as well as a 2.3 kW PV array. A heat exchanger circulated glycol liquid between the feed water of the RO system and the PVT solar panel array. The heat exchange loop worked by capturing heat from the PVT panel array and heating the feed water to the RO system.

The first objective of this study was to assess the difference in energy production of the PVT solar panel system when the heat exchanger was on vs when it was off. When evaluating the statistical distribution of the operating temperature, the the median daily temperature of the PVT panels was 7.6 °F lower when cooled compared to when the heat exchange system was off. With respect to energy production during the 8-week period (8/25/23-10/26-23), mean and median values showed an increase in energy production when the heat exchanger was on. Accounting for the PV baseline difference of 0.8%, an increase of 7.1% was observed due to operation of the heat exchange which corresponds to nearly 1% increase in energy production observed per °F cooled.

The second objective of this study was to assess whether the increase in feed water temperature from the heat exchanger would produce a significant increase in total water production. Feed water temperatures increased by an average of 3.82°F during operation of the heat exchanger, and daily permeate production showed a 0.8% and 0.4% increase in mean and median values, respectively.

The third objective of this study was to assess the change in water quality when the RO feed water was heated. Analysis of the feed water conductivity showed a negligible difference between on and off heat exchange periods, providing confidence in the consistency of our feed water quality throughout the 8-week evaluation period. Permeate conductivity showed an increase of 0.1% in mean values and 0.2% in median values between off and on heat exchange periods, so there was a negligible difference in the permeate conductivity. Furthermore, no substantial differences were observed with respect to individual ion rejection for calcium, magnesium, sodium, chloride, sulfate, and alkalinity.

For the testing conditions the system was evaluated under during the 8-week period, while an increase in PVT energy production of 7.1% was observed due to heat exchange, no significant increase in water production was observed with the coupled PVT-RO desalination system. Future work could evaluate the existing PVT system with a smaller RO system to impart a greater temperature difference and observe whether there is significant difference in the parameters identified in the objectives of this study.

To improve future evaluation of this system, consistent daily monitoring of system data is recommended to ensure issues are identified and resolved without major interruptions to operation and data collection. Performance ratio analysis of the PV and PVT systems could provide beneficial data by normalizing the PV and PVT energy production through a standard process.

REFERENCES

Goh, P. S., Matsuura, T., Ismail, A. F., & Ng, B. C. (2017). The Water–Energy Nexus: Solutions towards Energy-Efficient Desalination. In *Energy Technology* (Vol. 5, Issue 8, pp. 1136–1155). Wiley-VCH Verlag. https://doi.org/10.1002/ente.201600703

He, C., Liu, Z., Wu, J., Pan, X., Fang, Z., Li, J., & Bryan, B. A. (2021). Future global urban water scarcity and potential solutions. *Nature Communications*, *12*(1). https://doi.org/10.1038/s41467-021-25026-3

Kabir, E., Kumar, P., Kumar, S., Adelodun, A. A., & Kim, K. H. (2018). Solar energy: Potential and future prospects. In *Renewable and Sustainable Energy Reviews* (Vol. 82, pp. 894–900). Elsevier Ltd. https://doi.org/10.1016/j.rser.2017.09.094

Mekonnen, M. M., & Hoekstra, A. Y. (2016). Sustainability: Four billion people facing severe water scarcity. *Science Advances*, *2*(2). https://doi.org/10.1126/sciadv.1500323

Tiwari, G. N., Mishra, R. K., & Solanki, S. C. (2011). Photovoltaic modules and their applications: A review on thermal modelling. In *Applied Energy* (Vol. 88, Issue 7, pp. 2287–2304). Elsevier Ltd. https://doi.org/10.1016/j.apenergy.2011.01.005

Waqar Akram, M., Li, G., Jin, Y., & Chen, X. (2022). Failures of photo. In *Applied Energy* (Vol. 313). Elsevier Ltd. https://doi.org/10.1016/j.apenergy.2022.118822

GLOSSARY

BGNDRF   Brackish Groundwater National Desalination Research Facility

PV   Photovoltaic

PVT   Photovoltaic thermal

RO   Reverse Osmosis

VITA

Martin Chavarin was born and raised in El Paso, Texas. He is the youngest of five siblings. He obtained his Bachelor of Science degree in Civil Engineering in May 2017. As an undergraduate student, Martin maintained involvement in student organizations such as the American Society of Civil Engineers where he served as Vice President and Steel Bridge Captain. Martin Chavarin began pursuing a Master of Science degree in Environmental Engineering in the Spring of 2020. As a master student, Martin Chavarin served as the teaching assistant for the undergraduate Water and Wastewater Engineering course taught by Dr. Shane Walker. He also joined the Center for Inland Desalination Systems (CIDS) as a research assistant where he performed research in different water treatment projects including a desalination pilot located at the Brackish Groundwater National Desalination Research Facility. Martin looks forward to continuing a career in water treatment, with a focus on non-profit/charity work.